Space-charge wave excitation by superposition of static and moving interference patterns

B. Hilling,* T. Schemme, K.-M. Voit, H.-J. Schmidt, and M. Imlau
Department of Physics, University of Osnabrück, 49069 Osnabrück, Germany
(Received 13 August 2009; published 23 November 2009)

The optical excitation of space-charge waves (SCW) has been realized experimentally by superposition of static and moving light interference patterns with $Bi_{12}GeO_{20}$ as an example. A clear resonance behavior of the ac detected in an external electric circuit, as well as an inverse dispersion law, is verified, and a low frequency signal due to a modulation of the photoconductivity appears. The results are compared to the classical method using an oscillating light pattern for excitation. The optimized method allows for the detection of the charge carriers participating in SCW formation and yields an excitation of higher quality.

DOI: 10.1103/PhysRevB.80.205118 PACS number(s): 71.45.Lr, 72.20.Jv, 42.65.−k, 42.70.Nq

I. INTRODUCTION

Space-charge waves (SCW) are eigenmodes of spatial temporal oscillations of a space-charge density that can appear in semi-insulating semiconductors in an external electric field.[1] They are used to investigate either light-assisted charge transport properties or nonlinearities related to SCW-superposition. SCW can be generated optically, for instance, by an interference pattern moving collinear to a static electric field.[2] A photodetector for microwave signals based on this technique was proposed by Dolfi *et al.* and Hundhausen *et al.*[3,4] Alternatively, the semi-insulating sample can be exposed to a static interference pattern at the presence of an alternating electric field.[5] Polar electro-optic materials allow for the detection of the generated SCW by light diffraction at the spatially modulated space-charge fields, which are transferred to a modulation of the refractive index via the Pockels effect. In order to study SCW in nonelectro-optic crystals like silicon carbide,[6] the sample can be exposed to an oscillating light interference pattern in the presence of a static electric field.[7] For low oscillation amplitudes $\theta \ll 1$ the oscillating pattern can be separated mathematically into one static and two counterpropagating patterns of equal spatial frequency K

$$W(x,t) = W_0 \cdot \left[1 + m\cos(Kx) - \frac{m\theta}{2}\sin(Kx + \Omega t) - \frac{m\theta}{2}\sin(Kx - \Omega t) \right], \quad (1)$$

with W_0 being the total light intensity, m is the modulation depth, and Ω is the frequency of oscillation [Eq. (1) in Ref. 7]. Due to the effect of spatial rectification,[8] where the static grating interacts with the moving one, an alternating current appears inside the sample. This current can be detected in an appropriate electrical circuit, i.e., SCW generation with an oscillating light pattern provides electrical detection of SCW. In recent years, this method uncovered several insights to the physics of SCW, for example, the uncommon case of trap-recharging waves (TRW) with a linear dispersion law,[9] the interaction of SCW with magnetic fields,[10,11] and the effects of optical interband excitation.[12] However, these studies were affected by the following systematic limitations: (i) the oscillating pattern has no distinctive direction of motion, i.e., the sign of the charge carriers participating in SCW formation cannot be determined. This hinders the allocation of resonance signals to electrons and holes as, for instance, found in the case of interband excitation.[12] (ii) The oscillating light pattern consists of a spectrum of waves with different phase velocities $v_i = \Omega_i / K$. This results in the excitation of a bunch of charge density oscillations with phase velocities v_i, while resonant SCW generation results from the only part of the spectrum with $v_i = v_R = \Omega_R / K$, where Ω_R denotes the SCW-eigenfrequency. The interaction of these oscillations with each other results in the appearance of several ac signals with different frequencies yielding a broadened resonance peak. Moreover, the oscillating pattern can match the phase velocity v_R of the resonance mode only for a very short time, i.e., the oscillating pattern provides a discontinuous excitation. (iii) So far, the theoretical analysis is restricted to the cases of a low modulation amplitude θ. A more general analysis including the consideration of higher modulation amplitudes becomes very extensive, because higher orders of the Taylor expansion of the oscillating interference pattern have to be included.

Obviously, we can overcome these limitations simultaneously by a simple, but very effective optimization of the oscillation method as follows: instead of the generation of one static and two counterpropagating patterns by an oscillating interference pattern, we expose the sample to two discrete light patterns; one static and one moving pattern of the same spatial frequency, whereby we can particularly adjust the direction of motion and phase velocity of the latter. The discrete superposition of these two patterns avoids approximations for its description, keeping the effect of spatial rectification. Furthermore, the sign of the charge carriers involved in the photoelectric transport mechanisms can be determined, since the direction of motion of the pattern with respect to the electric field is adjustable. Finally, the incident moving light pattern consists of only one phase velocity v so that a high quality factor for resonance can be expected. Such SCW-generation scheme was addressed theoretically by Kleinert within a different framework related to the analysis of electron and hole dynamics.[13]

The aim of the present paper is to experimentally establish the method for SCW excitation using static and moving patterns and to highlight the advantages we found by comparison with the results obtained with a reference sample with the method using an oscillating pattern. By this means,

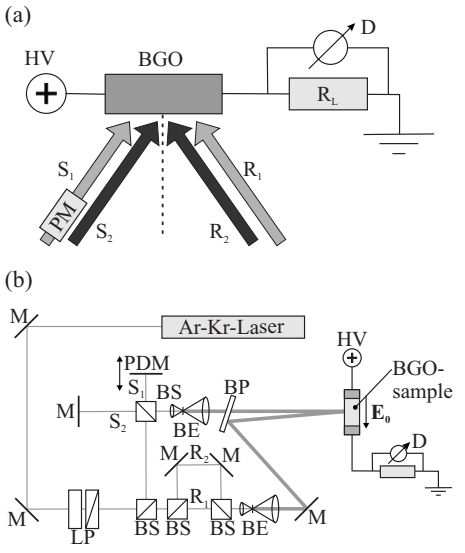

FIG. 1. (a) Experimental approach; $R_{1,2}$: reference beams, $S_{1,2}$: signal beams, PM: phase modulator, HV: high-voltage source, R_L: loading resistor, D: detection system including lock-in amplifier. (b) Scheme of the experimental setup with an Ar^+-Kr^+-laser at $\lambda = 514$ nm as pump source; LP: half-wave plate and polarizer, BS: beam splitters, PDM: piezo driven mirror, BE: beam expanders, BP: beam splitter plate, M: mirrors, $\mathbf{E_0}$: applied electric field.

the present article will verify that this concept (i) is capable of SCW generation with a high quality factor and (ii) gives insights to features of SCW, as well as of photoelectric processes in semi-insulating semiconductors. With $Bi_{12}GeO_{20}$ as an example, it will be shown that all expectations of the optimized method are verified by the experiments. Furthermore, a low frequency signal is uncovered, which overlays with the SCW resonance spectra. This signal can be attributed unambiguously to a temporal oscillation of the photoconductivity induced by the specific temporal properties of a light pattern generated by the superposition of one static and one moving pattern.

II. EXPERIMENTAL APPROACH, SETUP, AND SAMPLE

For excitation of SCW, the optical setup sketched in Fig. 1(a) has been developed. Two mutually decoherent sets of reference and signal beams $R_{1,2}$ and $S_{1,2}$ are adjusted so that they propagate collinear with respect to each other. The four beams generate two interference patterns with the same spatial frequency $|\mathbf{K}| = K = 2\pi\Lambda^{-1}$ and same direction of the wave vector $\mathbf{K}$ parallel to the applied electric field $\mathbf{E_0}$, where Λ denotes the spacing of the interference pattern. The beams S_2 and R_2 generate a static pattern $W_s(x)$; due to a linear phase modulation of S_1 with the phase modulation frequency Ω, the beams S_1 and R_1 generate a moving pattern $W_m(x,t)$ with the phase velocity $v = \Omega K^{-1}$. The two patterns can be expressed by

$$W_s(x) = W_1 \cdot [1 + m\cos(Kx)] \quad \text{and} \tag{2}$$

$$W_m(x,t) = W_1 \cdot [1 + m\cos(Kx + \Omega t)], \tag{3}$$

with W_1 being the light intensity and m is the modulation depth. Due to the decoherent superposition, the resulting pattern is given by the sum of W_s and W_m

$$W(x,t) = W_0 \cdot \left[1 + \frac{1}{2}m\cos(Kx) + \frac{1}{2}m\cos(Kx + \Omega t)\right], \tag{4}$$

where the total light intensity is $W_0 = 2 \cdot W_1$. This equation is quite similar to Eq. (1) derived for the oscillating interference pattern in the introduction, but there are two important differences: (i) Eq. (4) contains only one moving pattern instead of two counterpropagating ones. (ii) The equation for the oscillating interference pattern [Eq. (1)] is derived with the condition $\theta \ll 1$, while Eq. (4) represents the real incident illumination at the sample via the superposition of the static and the moving pattern.

The experimental implementation is presented in Fig. 1(b). The light of an Ar^+-Kr^+-Laser at 514 nm is split into four beams. Two of the beams are delayed equally in respect of their optical paths in order to create two mutually decoherent pairs of beams. All beams are expanded and spatially filtered to provide a homogeneous illumination of the sample. Phase modulation of S_1 is realized with a piezo driven mirror, i.e., the direction of movement of the pattern can be chosen by using an appropriate slope of the phase modulation signal. The modulation depth m of the interference patterns can be varied by adjusting the intensity ratio of signal and reference beams. For the experiments, the intensities of both reference beams and those of the signal beams are adjusted to $I_{R_1} = I_{R_2}$ and $I_{S_1} = I_{S_2}$, i.e., both interference patterns exhibit the same light intensity $W_1 = I_R + I_S$ and the same modulation depth $m = 2 \cdot \sqrt{I_R I_S}/(I_R + I_S)$. The sample is connected to a high-voltage source to provide the static electric field in the range of $(1-11)$ kV cm^{-1}.

The illumination with the light pattern leads to a charge density modulation inside the sample. The interaction of the static part of this modulation with the moving one yields an alternating current I_1.[8] This current is detected electrically with a lock-in amplifier as a function of the modulation frequency. Detailed information about the technique used can be found in Ref. 6.

The experimental setup used for excitation with the oscillating interference pattern is the same as described in Ref. 6 with a different pump beam wavelength of 514 nm.

The sillenite $Bi_{12}GeO_{20}$ (BGO) of Ref. 14 (notation BGO 2.1 in Ref. 15) was chosen as a sample. It is of size $2.0 \times 2.4 \times 3.7$ mm^3 ($[110] \times [001] \times [1\bar{1}0]$), the light propagation was along the [110] axis, the grating wave vector and the applied field were directed along the $[1\bar{1}0]$ axis, and the polarization of the light was adjusted parallel to the [001] axis. Electrodes made of conductive silver paste were deposited on the $(1\bar{1}0)$ faces to connect it to the outside electrical circuit. All results shown are obtained using a total light intensity of $W_0 = 30$ mW cm^{-2}.

III. EXPERIMENTAL RESULTS

Figure 2 shows typical signals of the amplitude of the ac I_1 normalized to its maximum value as a function of the phase modulation frequency Ω. The experimental results of the method using static and moving patterns are presented

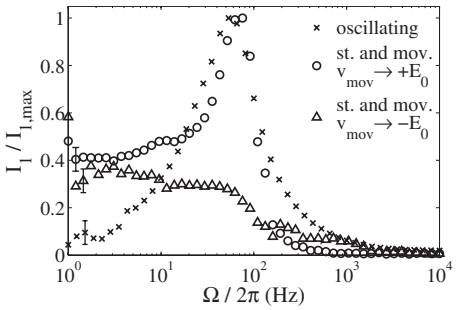

FIG. 2. Dependence of I_1 on Ω for $K=3.6\cdot10^3$ cm^{-1} and $E_0=4.3$ kV cm^{-1} with $\lambda=514$ nm, $W_0=30$ mW cm^{-2}, $m=0.45$, and $\theta=0.3\pi$. The data of static and moving patterns with reversed direction of the moving pattern (△) are normalized to the ac at resonance with the moving pattern and electric field having the same direction.

for the movement of the moving pattern in (○) and against (△) the direction of the electric field. The data of the oscillating pattern (×) are shown for a phase modulation amplitude of $\theta=0.3\pi$. Exemplarily, all results are given for a spatial frequency $K=3.6\cdot10^3$ cm^{-1} and an electric field $E_0=4.3$ kV cm^{-1}. One can find resonant behavior for the excitation with static and moving patterns at a frequency $\Omega_R/2\pi$ of about 70 Hz only if the directions of electric field and movement of the pattern coincide (○). For very low frequencies $\Omega/2\pi$ less than 10 Hz, an ac of about $0.4\cdot I_1(\Omega_R)$ persists. The resonance vanishes, if the direction of movement of the pattern is inverted (△). Here, only the low frequency signal remains up to frequencies of ≈100 Hz. With the oscillating pattern $\Omega_R/2\pi=60$ Hz is slightly lower and no low frequency signal occurs. The comparison of both resonances shows that the width of the resonance function is decreased for the presented experimental approach.

The presence of SCW is verified by the dispersion behavior, i.e., the dependence of Ω_R on K, as depicted in Fig. 3, here, for $E_0=7.6$ kV cm^{-1}. Obviously, the resonance frequency drops with increasing spatial frequency for both methods used. A comparable behavior is found for the dependence of the resonance frequency on the applied electric field (not depicted for reasons of clarity). The solid line in Fig. 3 is a fit of the data of static and moving patterns to $\Omega_R=(\tau_M\cdot\mu\tau\cdot K\cdot E_0)^{-1}$ [Eq. (29) in Ref. 16], yielding

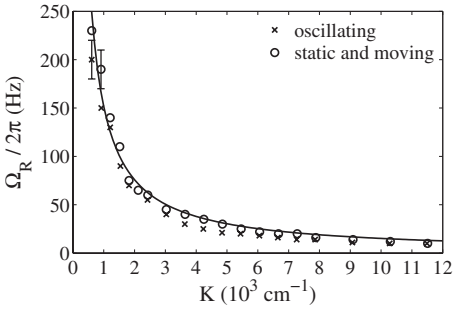

FIG. 3. Dependence of Ω_R on K for $E_0=7.6$ kV cm^{-1} with $\lambda=514$ nm, $W_0=30$ mW cm^{-2}, $m=0.45$, and $\theta=0.3\pi$. The solid line is a fit of Eq. (29) in Ref. 16 to the data of static and moving patterns with $\tau_M\cdot\mu\tau=1.4\cdot10^{-14}$ m^2 s V^{-1}.

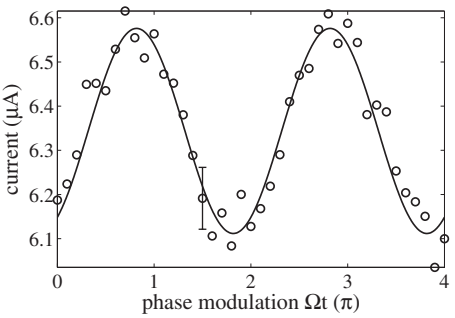

FIG. 4. Modulation of the dc current in dependence on the phase modulation Ωt for $W_0=30$ mW cm^{-2}, $m=0.45$, $K=3.6\cdot10^3$ cm^{-1}, and $E_0=4.3$ kV cm^{-1}. The time interval between increasing Ωt and obtaining the current is 5 s. The line is a guide to the eye.

$\tau_M\cdot\mu\tau=(1.4\pm0.2)\cdot10^{-14}$ m^2 s V^{-1}. Here, $\mu\tau$ is the product of mobility and lifetime of the charge carriers and τ_M is the Maxwell relaxation time. The equation is derived for the conditions that $\mu\tau$ and the effective trap density are simultaneously large and $L_0\cdot K>1$ with $L_0=\mu\tau\cdot E_0$ being the drift length of the charge carriers in the applied electric field.

To verify the persistence of a low frequency signal for frequencies $\Omega\to0$, an additional data point for $\Omega/2\pi=10^{-2}$ Hz is determined by the following modification of the measurement: the dc current is detected during application of a static electric field and exposure of the sample to two static, mutually decoherent sinusoidal light patterns of the same spatial frequency; then the relative phase shift Ωt of one of the patterns with respect to the other is increased stepwise. A dc current appears, which is determined in steps of $\pi/10$ for a duration of 5 s for each step with a common dc voltmeter. This dc current is plotted as a function of Ωt as depicted in Fig. 4. Obviously, the dc current is modulated with an amplitude of (0.23 ± 0.04) μA around a mean value of (6.35 ± 0.03) μA with a periodicity of 2π.

Figure 5(a) shows the ac $I_1(\Omega_R)$ at resonance in dependence on the spatial frequency K for $E_0=7.6$ kV cm^{-1} normalized to the maximal ac, respectively. Both dependences exhibit a maximum, but located at different spatial frequencies of $K\approx6\cdot10^3$ cm^{-1} for static and moving patterns and $K\approx1\cdot10^3$ cm^{-1} for the oscillating pattern. The dependence of $I_1(\Omega_R)$ on the applied electric field E_0 for $K=6.1\cdot10^3$ cm^{-1} is presented in Fig. 5(b). For both methods the ac at resonance is proportional to the applied electric field.

IV. DISCUSSION

Figure 2 shows clear resonance behaviors of both methods used; the dispersion of the resonance (Fig. 3) reflects a significant drop of the resonance frequency Ω_R with increasing spatial frequency K. Equivalent behavior is found as a function of the applied electric field E_0, so that the dependences obey the dispersion law $\Omega_R=(\tau_M\cdot\mu\tau\cdot K\cdot E_0)^{-1}$ [Eq. (29) in Ref. 16]. This dispersion law is characteristic for the generation of TRW, i.e., the resonance signals found have to be assigned to TRW. Assuming $\mu\tau=1.6\cdot10^{-11}$ m^2 V^{-1} from Ref. 14, one can find $\tau_M=(8.8\pm1.3)\cdot10^{-4}$ s from the fit to

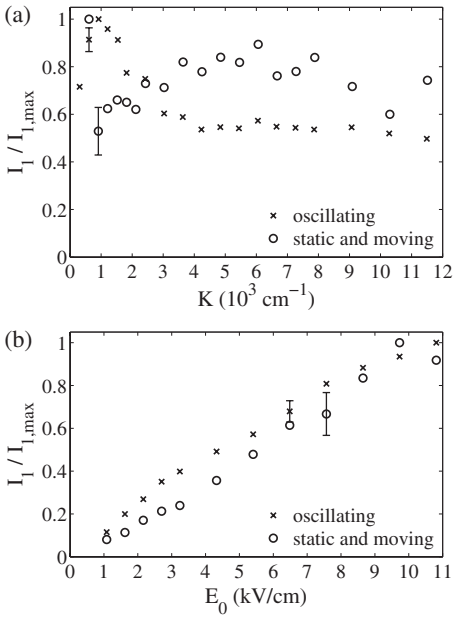

FIG. 5. (a) Dependence of $I_1(\Omega_R)$ on K for $E_0=7.6$ kV cm^{-1} with $\lambda=514$ nm, $W_0=30$ mW cm^{-2}, $m=0.45$, and $\theta=0.3\pi$. (b) Dependence of $I_1(\Omega_R)$ on E_0 for $K=6.1\cdot10^3$ cm^{-1} with $\lambda=514$ nm, $W_0=30$ mW cm^{-2}, $m=0.45$, and $\theta=0.3\pi$.

the experimental data shown in Fig. 3. Both results, the presence of the resonance signal and the dispersion behavior, give clear evidence that the discrete superposition of a static and a moving pattern is appropriate for the generation of SCW.

Beyond that, Fig. 2 shows qualitative differences between the results obtained with the two methods. The most significant one can be found at low modulation frequencies. Here, the static and moving patterns generate an ac with a constant amplitude of (0.17 ± 0.02) μA in the low frequency region. Figure 4 shows that this signal remains even for $\Omega/2\pi=10^{-2}$ Hz with an amplitude of (0.23 ± 0.04) μA, i.e., the amplitudes agree quite well with each other. It follows that the signal is stable for $\Omega\rightarrow0$. This low frequency signal can be attributed to the temporal oscillation of the shape of the resulting pattern described by Eq. (4). Obviously, its shape depends on the phase modulation Ωt: If $\Omega t=\pi,3\pi,\ldots$, the two initial patterns superimpose destructively and the illumination becomes homogeneous; for a case $\Omega t=0,2\pi,\ldots$, the resulting pattern exhibits maximum modulation depth. This dependence of the fringe pattern on Ωt affects the detected current as a function of Ωt as follows: in the case of negligible thermal excitation and not too high light intensities, the density of charge carriers in the conduction band is proportional to the light intensity,[17] i.e., the conductivity is proportional to the intensity of light. Thus, one can expect that the conductivity that is the sum of dark and photoconductivity will depend on Ωt, which is verified by Fig. 4. The sample exhibits the highest current, i.e., the highest conductivity, if the light patterns are adjusted to a mutual phase shift of $\pi,3\pi,\ldots$, while for $0,2\pi,\ldots$ the conductivity is the lowest. This can be specified by illuminating the sample homogeneously or with an interference pattern of the same total light intensity, where the higher conductivity can be found for homogeneous illumination. Hence, the movement of the moving pattern over the static one yields an ac for $\Omega\rightarrow0$ due to the modulation of the photoconductivity. Because the externally determined current is modulated also in the steady state, the origin of the ac at $\Omega\rightarrow0$ cannot be assigned to the interaction of the static and the moving charge gratings inside the sample. This explains why the low frequency signal remains when the direction of movement of the moving pattern is inverted. Here, only the resonance vanishes ($\triangle$ in Fig. 2), because the conditions for SCW generation are not fulfilled in our specific case. If $\Omega\gg1$, no ac occurs, because the decay of the space-charge field and therefore, also of the charge density modulation follows an exponential law with a characteristic time τ_{sc}.[18] In the case $\Omega^{-1}\ll\tau_{sc}$, the charge density modulation does not decay significantly during one period of movement of the pattern, i.e., the conductivity remains.

In contrast, the oscillating pattern generates no alternating current for very low frequencies. This is due to the fact that this light pattern does not change its overall shape as a function of time, but only with respect to its phase. Because the product $Kl\gg1$ holds for our sample of length l, the photoconductivity is independent on the phase and, thus, of frequency Ω.

The ratio of eigenfrequency and damping of a wave is the so-called quality factor Q. Comparing the resonances in Fig. 2, one can find that the resonance frequency using static and moving patterns is slightly shifted to higher frequencies under comparable experimental conditions than the ones using an oscillating pattern. Moreover, the width of the resonance $\Delta\Omega$ at $I_1(\Omega_R)/\sqrt{2}$ is smaller, i.e., using the introduced pattern for SCW generation is connected with a lower damping of the wave. This means that an enhancement of the quality factor is revealed. For the data shown here, $Q=\Omega_R/\Delta\Omega=1.3$ for the optimized and $Q=0.9$ for the classical light pattern, i.e., the quality factor is increased by nearly 50%. As a qualitative explanation for this effect, we like to consider that the method uses a discrete superposition of two patterns. If resonance occurs, the moving pattern exhibits a constant phase velocity $v_R=\Omega_R/K$ equal to the velocity of the SCW. In contrast, the oscillating pattern exhibits an oscillating velocity, because the fringe pattern is continuously accelerated and decelerated. The velocity of the pattern will hence coincide with the velocity of the SCW only for a short time. Moreover, due to the different phase velocities of the pattern different modes of charge density oscillations will be excited. It cannot be excluded that these modes interact with each other and provide unwanted ac signals that also might contribute to the detected ac. This will broaden the SCW resonance generated with the oscillating pattern significantly. Theoretically, the maximum possible quality factor depends only on material parameters.[19] In GaAs and CdTe, Q_{max} can reach values of 100 while for sillenites $Q_{max}\approx10$.[19] Hence, although the quality factor already has been increased significantly by our SCW generation scheme, the Q factor may be further improved in future measurements.

The determination of the sign of the charge carriers being involved in generation of SCW is possible only for the excitation with static and moving patterns. Resonant excitation occurs if the phase velocity of the incident pattern coincides

with the phase velocity of the SCW.[20] Here, resonant excitation can be observed for the moving pattern propagating in direction of the applied electric field (cf. Figure 2). For the case of TRW, where $\Omega_R \propto K^{-1}$, group and phase velocity are contrary, i.e., in this case the group velocity is contrary to the electric field. This means the charge carriers are electrons, which is consistent with the fact that the dominating photoinduced charge carriers in BGO are electrons.[21]

The Figs. 5(a) and 5(b) show the dependences of I_1 at Ω_R on K and E_0. While $I_1(\Omega_R) \propto E_0$ for both methods, the dependences of $I_1(\Omega_R)$ on K differ. To explain and analyze these accordances and differences, the theoretical investigation of the dependence of I_1 on Ω becomes necessary, i.e., a formula for $I_1(\Omega)$ has to be developed from an appropriate theoretical concept taking the SCW generation by the superposition of static and moving patterns into account. Nevertheless, no significant new dependences appear; i.e., the method can be applied comprehensively, as it was realized for the oscillating pattern so far.

Moreover, not only the first harmonic of the alternating current I_1 can be investigated. For instance, other nonlinear interaction of space-charge waves giving rise to spatial doubling, overall doubling, or overall rectification can be expected. These interactions have been studied already for the excitation with the oscillating interference pattern.[14,22] In particular, the interaction of the moving and static gratings as well as their complex conjugated terms have to be considered.

V. CONCLUSION

In conclusion, we have presented a method for the optical excitation of SCW by the superposition of one static and one moving pattern. It is shown that this type of light pattern is capable to excite SCW with the following features: (i) the quality factor of resonance is significantly larger compared with classical methods using an oscillating light pattern, (ii) the sign of charge carriers participating in SCW generation can be determined, and (iii) a low frequency signal occurs, which is not related to SCW, but reflects the frequency dependence of photoconductivity.

ACKNOWLEDGMENTS

Financial support by the DFG (Deutsche Forschungsgemeinschaft) within the graduate college 695 "Nonlinearities of Optical Materials" is gratefully acknowledged. Especially, the authors would like to thank M. P. Petrov from the Ioffe Institute in St. Petersburg, Russia, for fruitful discussions during his visit in March 2008.

*buhillin@uos.de

[1] R. F. Kazarinov, R. A. Suris, and B. I. Fuks, Sov. Phys. Semicond. **6**, 500 (1972).
[2] J. P. Huignard and A. Marakchi, Opt. Commun. **38**, 249 (1981).
[3] D. Dolfi, T. Merlet, A. Mestreau, and J. P. Huignard, Appl. Phys. Lett. **65**, 2931 (1994).
[4] M. Hundhausen, L. Ley, and C. Witt, Appl. Phys. Lett. **69**, 1746 (1996).
[5] S. I. Stepanov and M. P. Petrov, Opt. Commun. **53**, 292 (1985).
[6] M. Lemmer, B. Hilling, M. Wöhlecke, M. Imlau, A. A. Lebedev, V. V. Bryksin, and M. P. Petrov, Eur. Phys. J. B **60**, 9 (2007).
[7] M. P. Petrov, V. V. Bryksin, F. Rahe, C. E. Rüter, and E. Krätzig, Opt. Commun. **227**, 183 (2003).
[8] M. P. Petrov, A. P. Paugurt, V. V. Bryksin, S. Wevering, and E. Krätzig, Phys. Rev. Lett. **84**, 5114 (2000).
[9] M. P. Petrov, V. V. Bryksin, K. Shcherbin, M. Lemmer, and M. Imlau, Phys. Rev. B **74**, 085202 (2006).
[10] M. P. Petrov, V. V. Bryksin, M. Lemmer, B. Hilling, M. Wöhlecke, and M. Imlau, Phys. Rev. B **76**, 033202 (2007).
[11] D. V. Petrov, M. P. Petrov, B. Hilling, M. Lemmer, and M. Imlau, Appl. Phys. B: Lasers Opt. **95**, 483 (2009).
[12] M. P. Petrov, V. V. Bryksin, B. Hilling, M. Lemmer, and M. Imlau, Phys. Rev. B **78**, 085121 (2008).
[13] P. Kleinert, J. Appl. Phys. **97**, 073711 (2005).
[14] M. P. Petrov, V. V. Bryksin, H. Vogt, F. Rahe, and E. Krätzig, Phys. Rev. B **66**, 085107 (2002).
[15] H. Vogt, K. Buse, H. Hesse, E. Krätzig, and R. R. Garcia, J. Appl. Phys. **90**, 3167 (2001).
[16] V. V. Bryksin and M. P. Petrov, Phys. Solid State **48**, 1234 (2006).
[17] K. Buse, Appl. Phys. B: Lasers Opt. **64**, 273 (1997).
[18] M. P. Petrov, S. I. Stepanov, and A. V. Khomenko, *Photorefractive Crystals in Coherent Optical Systems* (Springer-Verlag, Berlin, 1991).
[19] B. I. Sturman, M. Mann, J. Otten, and K. H. Ringhofer, J. Opt. Soc. Am. B **10**, 1919 (1993).
[20] V. V. Bryksin, P. Kleinert, and M. P. Petrov, Phys. Solid State **46**, 1613 (2004).
[21] R. E. Aldrich, S. L. Hou, and M. L. Harvill, J. Appl. Phys. **42**, 493 (1971).
[22] M. P. Petrov, V. V. Bryksin, S. Wevering, and E. Krätzig, Appl. Phys. B: Lasers Opt. **73**, 699 (2001).